

Aristolochic Acids Induce Chronic Renal Failure with Interstitial Fibrosis in Salt-Depleted Rats

FRÉDÉRIC D. DEBELLE,* JOËLLE L. NORTIER,[†] ERIC G. DE PREZ,*
CHRISTIAN H. GARBAR,[‡] ANNE R. VIENNE,[‡] ISABELLE J. SALMON,[‡]
MONIQUE M. DESCHODT-LANCKMAN,* and JEAN-LOUIS VANHERWEGHEM[†]

*Laboratory for Research on Peptide Metabolism, Faculty of Medicine, and Departments of [†]Nephrology and [‡]Pathology, Erasme Hospital, Université Libre de Bruxelles, Brussels, Belgium.

Abstract. Chinese-herb nephropathy (CHN) is a rapidly progressive renal fibrosis associated with the intake of a Chinese herb (*Aristolochia fangchi*) containing nephrotoxic and carcinogenic aristolochic acids (AA). This study attempted to reproduce the main features of human CHN (renal failure, tubular atrophy, and interstitial fibrosis) in a rat model similar to that of cyclosporin-induced nephropathy. Salt-depleted male Wistar rats received daily subcutaneous injections of either 1 mg/kg body wt AA (low-dose AA group), 10 mg/kg body wt AA (high-dose AA group), or vehicle (control group) for 35 d. On days 10 and 35, assessment of renal function, measurements of urinary excretion of glucose, protein, and leucine aminopeptidase, and histologic analyses were performed (six

rats euthanized/group). High-dose AA induced glucosuria, proteinuria, and elevated serum creatinine levels and reduced leucine aminopeptidase enzymuria on days 10 and 35, whereas low-dose AA had no significant effect. Tubular necrosis associated with lymphocytic infiltrates (day 10) and tubular atrophy surrounded by interstitial fibrosis (day 35) were the histologic findings for the high-dose AA-treated rats. In both AA groups, urothelial dysplasia was also observed, as well as fibrohistiocytic sarcoma at the injection site. A short-term model of AA-induced renal fibrosis was established in salt-depleted Wistar rats. These results support the role of AA in human CHN and provide a useful model for examination of the pathophysiologic pathways of renal fibrosis.

Chinese-herb nephropathy (CHN), a progressive interstitial nephropathy, has been observed among women after the intake of weight-reducing pills containing a Chinese herb, namely *Stephania tetrandra* (1). Phytochemical analyses of herb powder of so-called *S. tetrandra* resulted in the identification of aristolochic acids (AA) instead of tetrandrine (2), confirming the replacement of *S. tetrandra* (han fangji) by *Aristolochia fangchi* (guang fangji). Exposure to AA was confirmed by the detection of AA-DNA adducts in kidney tissue samples (3,4).

Interstitial fibrosis is the typical histologic finding initially observed in the renal superficial cortex (5,6). Moreover, a high prevalence of urothelial carcinoma was reported among patients with end-stage CHN (4,7).

AA are known for their nephrotoxic effects in rodents, as well as for their carcinogenic and mutagenic properties (8). Administration of AA to rats resulted in acute tubular necrosis (9) or plurifocal cancer lesions (10,11). Initial attempts to experimentally reproduce the typical chronic interstitial lesions of CHN failed; AA administered orally (10 mg/kg, 5 d/wk, for 3 mo) to Wistar rats induced the expected tumors but not fibrosis or renal

insufficiency (12). Therefore, experiments were performed to evaluate another animal model. Intraperitoneal injections of 0.1 mg/kg AA (5 d/wk, for 17 to 21 mo) into New Zealand white (NZW) rabbits led to hypocellular interstitial fibrosis and urothelial atypia (13). Although these findings support the role of AA in the development of interstitial fibrosis, the length of AA exposure required in rabbits makes the experimental model less useful for the study of renal interstitial fibrosis.

As illustrated by experimental cyclosporin-induced nephropathy (14,15), salt depletion seems to be required for rats to develop renal fibrosis. Therefore, in this study, we developed a short-term model of AA-induced nephropathy in salt-depleted Wistar rats. We report these results in comparison with the renal abnormalities observed in human CHN.

Materials and Methods

Experimental Protocol

Sixty-six male Wistar rats (age, 4 wk; weight, approximately 100 g; Elevage Janvier, Le Genest Saint-Isle, France) were housed in the animal care facility of the Faculty of Medicine, Free University of Brussels (Brussels, Belgium). Groups of four or five animals were caged in a temperature-, humidity-, and light-controlled environment. After a 7-d acclimatization period, rats received a single dose of furosemide (4 mg/kg body wt, administered intraperitoneally; Hoechst Marion Roussel, Frankfurt, Germany). Animals were fed *ad libitum* a low-salt, normal-protein diet (0.05% sodium; Carfil Quality, Oud-Turnhout, Belgium) and were allowed free access to water throughout the study. One week later (on day 0), weight-matched rats were randomly assigned to three groups and received daily subcutaneous injections of the following drugs for 5 wk: a mixture of AA (Acros

Received August 27, 2001. Accepted October 20, 2001.

Correspondence to Dr. Joëlle L. Nortier, Department of Nephrology, Hôpital Erasme, Université Libre de Bruxelles, Route de Lennik, 808, B-1070 Brussels, Belgium. Phone: +32-2-555-3334; Fax: +32-2-555-6499; E-mail: jnortier@ulb.ac.be

1046-6673/1302-0431

Journal of the American Society of Nephrology

Copyright © 2002 by the American Society of Nephrology

Organics Co., Geel, Belgium) containing 40% AAI and 60% AAI, dissolved in polyethylene glycol (PEG) 400 (Fluka Chemie, Buchs, Switzerland) to a final concentration of 10 mg/ml and diluted in distilled water before subcutaneous injection at a dose of 1 mg/kg body wt AA (low-dose AA group, $n = 24$) or 10 mg/kg body wt AA (high-dose AA group, $n = 24$), or the vehicle only, consisting of a 50/50 mixture of PEG 400 and distilled water (control group, $n = 18$).

Body weights were recorded weekly, for adjustment of drug dosages. On days 10 and 35, six rats from each group were anesthetized with ether and euthanized by decapitation, for blood collection. Urine collection was performed the day before euthanasia, by housing the animals in metabolic cages. Blood samples were allowed to clot at room temperature, and the serum was separated by centrifugation at $1600 \times g$ for 15 min at 4°C and stored at -20°C until assayed. Urine samples were centrifuged at $1600 \times g$ for 15 min at 4°C for creatinine and leucine aminopeptidase (LAP) activity measurements. Kidney, lung, skin (injection site), and liver were quickly removed and fixed in 4% buffered formaldehyde for histologic analyses.

Surviving rats were observed daily, and their weights were recorded weekly. Euthanasia was performed on day 105. Approval of the protocol was provided by the Ethical Committee for Animal Care (Faculty of Medicine, Université Libre de Bruxelles).

Biochemical Measurements

Because of the very low serum creatinine levels in rats and the frequent overestimation of values resulting from interference with the Jaffé method, serum creatinine levels were measured by using a sensitive accurate HPLC method, which was adapted from that described by Xue *et al.* (16). Briefly, samples were deproteinized with the addition of acetonitrile and analyzed by HPLC using a strong cation-exchange column (Spherisorb 5- μm SCX column, 4.0×250 mm; Waters, Milford, MA). Elution was performed at room temperature by using a mobile phase of 9% acetonitrile in 40 mM ammonium phosphate (pH 5.3), at a flow rate of 1.0 ml/min. Absorbance was monitored at 230 nm. The within-run and between-day coefficients of variation were 2.7 and 3.0%, respectively ($n = 9$).

Urinary creatinine levels were measured by using the pseudokinetic Jaffé method (Roche Diagnostics Division, Brussels, Belgium). Urinary and plasma glucose levels were measured with a Cobas Mira autoanalyzer (Roche Diagnostics Division). Fractional excretion of glucose was determined as follows: fractional excretion = (urinary glucose concentration \times serum creatinine concentration)/(serum glucose concentration \times urinary creatinine concentration) (expressed as a percentage). Urinary protein levels were assayed by using the Bradford dye binding assay (17), with bovine serum albumin as a standard.

Determination of Proximal Tubular Brush Border LAP Activity

Urinary LAP enzymatic activity was measured with a spectrofluorometric assay, after 1:30 dilution of samples with 50 mM Tris-HCl buffer (pH 7.6). The synthetic substrate leucine-7-amido-4-methyl-coumarin (Bachem, Bubendorf, Switzerland) was incubated with the diluted samples at 37°C for 60 min. After the reaction had been stopped by sample heating at 95°C for 5 min, the fluorescence of free 7-amido-4-methyl-coumarin produced by the action of LAP was measured by using excitation and emission wavelengths of 367 and 440 nm, respectively. Results were expressed as micromoles of 7-amido-4-methyl-coumarin produced per millimole of urinary creatinine.

Histologic Evaluations

For conventional microscopy, fixed lung, liver, skin (injection site), and kidney samples embedded in paraffin were cut at 5 μm and stained

with hematoxylin and eosin, periodic acid-Schiff reagent, and Goldner's trichrome stain. Lung, skin, and liver were systematically evaluated for any abnormality. A complete section of the kidney was screened at a magnification of $\times 200$, and findings for the cortex were semiquantitatively scored by three independent observers (Drs. Debelle, Garbar, and Salmon). The scoring systems used were adapted from a previous report on the pathologic aspects of CHN (5) and were defined as follows: tubular atrophy: 0, normal tubules; 1, rare single atrophic tubule; 2, several clusters of atrophic tubules; 3, massive atrophy; tubular necrosis: 0, normal tubules; 1, rare single necrotic tubule; 2, several clusters of necrotic tubules; 3, massive necrosis; lymphocytic infiltrates: 0, absent; 1, few scattered cells; 2, groups of lymphocytes; 3, widespread infiltrate; interstitial fibrosis: 0, absent; 1, minimal fibrosis, with slight thickening of the tubular basal membrane; 2, moderate fibrosis, with focal enlargement of the interstitium; 3, severe fibrosis, with confluent fibrotic areas. Tubulointerstitial injury scores were defined as the sum of the four aforementioned scores.

The urothelium was systematically examined and graded for dysplasia according to World Health Organization criteria, as revised by Epstein *et al.* (18).

Statistical Analyses

Data are presented as means \pm SEM. Comparisons were made by one-way ANOVA. Significant ANOVA was followed by the *post hoc* Student-Newman-Keuls multiple-comparisons procedure. Nonparametric variables were analyzed with the Kruskal-Wallis ANOVA and the Mann-Whitney *U* test. Correlations between biologic and histologic data were assessed by calculating the Spearman correlation coefficient. A *P* value of <0.05 was considered significant.

Results

Body Weights and Survival Rates for Control, Low-Dose AA-Treated, and High-Dose AA-Treated Rats

As indicated in Figure 1, the mean body weights increased with similar patterns in the control and low-dose AA groups, whereas a significant breakdown in the high-dose AA group appeared on day 4 and persisted throughout the experimental

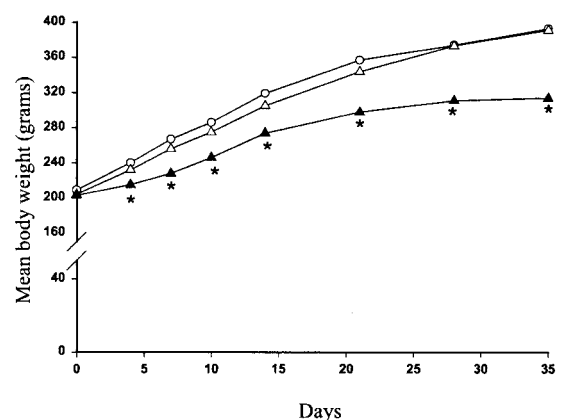


Figure 1. Time course of mean body weights for control (○), low-dose aristolochic acid (AA)-treated (1 mg/kg body wt) (△), and high-dose AA-treated (10 mg/kg body wt) (▲) rats. Results are the arithmetic means for 18 to 24 animals/group between day 0 and day 10 and 12 to 18 animals/group after euthanasia on day 10. * $P < 0.001$, high-dose AA-treated rats versus control rats.

protocol. One rat from the high-dose AA group was found dead in its cage on day 8.

Biologic Parameters for Control, Low-Dose AA-Treated, and High-Dose AA-Treated Rats

No difference in proteinuria was observed between the low-dose AA and control groups. In contrast, massive proteinuria was present in high-dose AA-treated rats, compared with control rats, on days 10 and 35. A slight increase in the fractional excretion of glucose was noted for the high-dose AA group on day 10, reaching a statistically significant value on day 35 (Table 1).

Mean serum creatinine levels are presented in Figure 2A. Identical values were observed for the low-dose AA and control groups. Renal insufficiency was observed for the high-dose AA group on day 10 ($P < 0.01$), and values were approximately 50% higher on day 35, compared with the control and low-dose AA groups ($P < 0.01$).

As indicated in Figure 2B, a significant decrease in LAP enzymuria was observed for the high-dose AA group on days 10 and 35, compared with the control and low-dose AA groups ($P < 0.01$). No difference between low-dose AA-treated rats and control rats was observed.

Histologic Findings and Scores

Examination of all lung and liver tissue samples revealed no significant abnormalities. Similarly, control rats treated with subcutaneous injections of PEG 400 did not exhibit renal morphologic alterations (Figure 3A).

In the low-dose AA group, no remarkable lesions were observed except slight tubular atrophy (day 10) and a few scattered lymphocytes (day 35) limited to the deep cortex. In contrast, major tubulointerstitial lesions were observed for the high-dose AA group. Tubular necrosis and atrophy, as well as lymphocytic infiltrates free of polymorphonuclear neutrophils, were observed on day 10 (Figure 3B). Tubular atrophy and lymphocytic infiltrates were still present on day 35 and were surrounded by severe interstitial fibrosis (Figure 3C). These lesions initially were predominant in the deep cortex and the outer medulla (day 10) and subsequently were also present in the medullary rays (day 35).

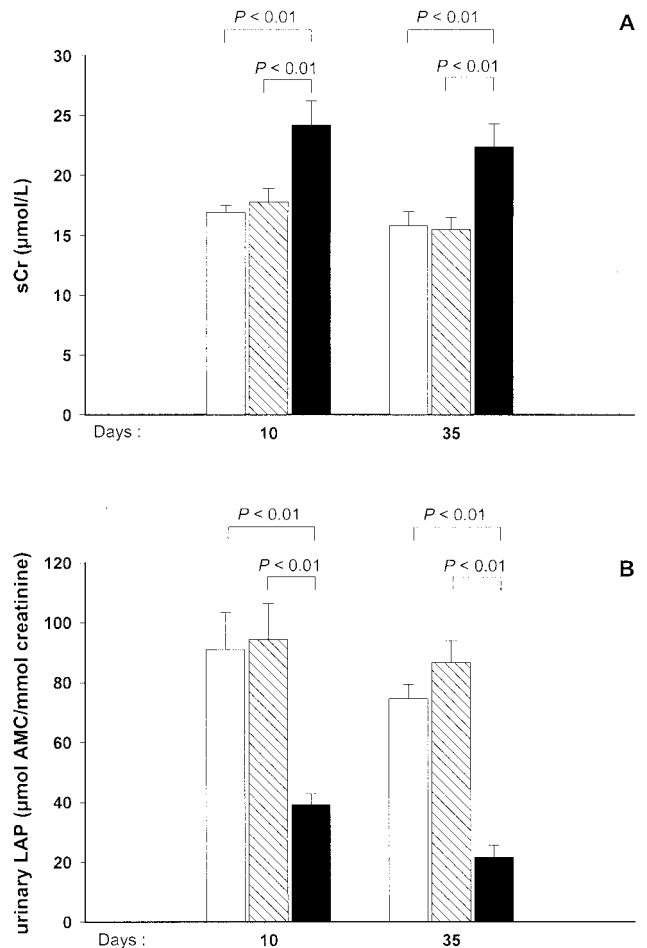


Figure 2. Serum creatinine levels (sCr) (A) and urinary leucine aminopeptidase (LAP) enzymatic activity (B) for control (□), low-dose AA-treated (1 mg/kg body wt) (▨), and high-dose AA-treated (10 mg/kg body wt) (■) rats on days 10 and 35. Data are the mean ± SEM for six rats/group. AMC, 7-amido-4-methyl-coumarin.

In the high-dose AA group, focal lymphocytic infiltrates without vasculitis were identified around interlobular vessels on days 10 and 35. Vascular changes, consisting of remodeling of smooth

Table 1. Fractional excretion of glucose and urinary excretion of proteins in control and AA-treated rats^a

	Day 10		Day 35	
	FE _{glucose} (%)	Urinary Protein Levels (g/mmol creatinine)	FE _{glucose} (%)	Urinary Protein Levels (g/mmol creatinine)
Control	0.16 ± 0.07	0.07 ± 0.01	0.05 ± 0.02	0.07 ± 0.01
Low-dose AA (1 mg/kg body wt)	0.19 ± 0.03	0.08 ± 0.01	0.08 ± 0.02	0.10 ± 0.01
High-dose AA (10 mg/kg body wt)	0.91 ± 0.37	0.17 ± 0.02 ^b	0.73 ± 0.20 ^c	0.25 ± 0.05 ^b

^a Data are the mean ± SEM for six rats/group. AA, aristolochic acids; FE_{glucose}, fractional excretion of glucose.

^b $P < 0.01$, compared with control rats.

^c $P < 0.05$, compared with control rats.

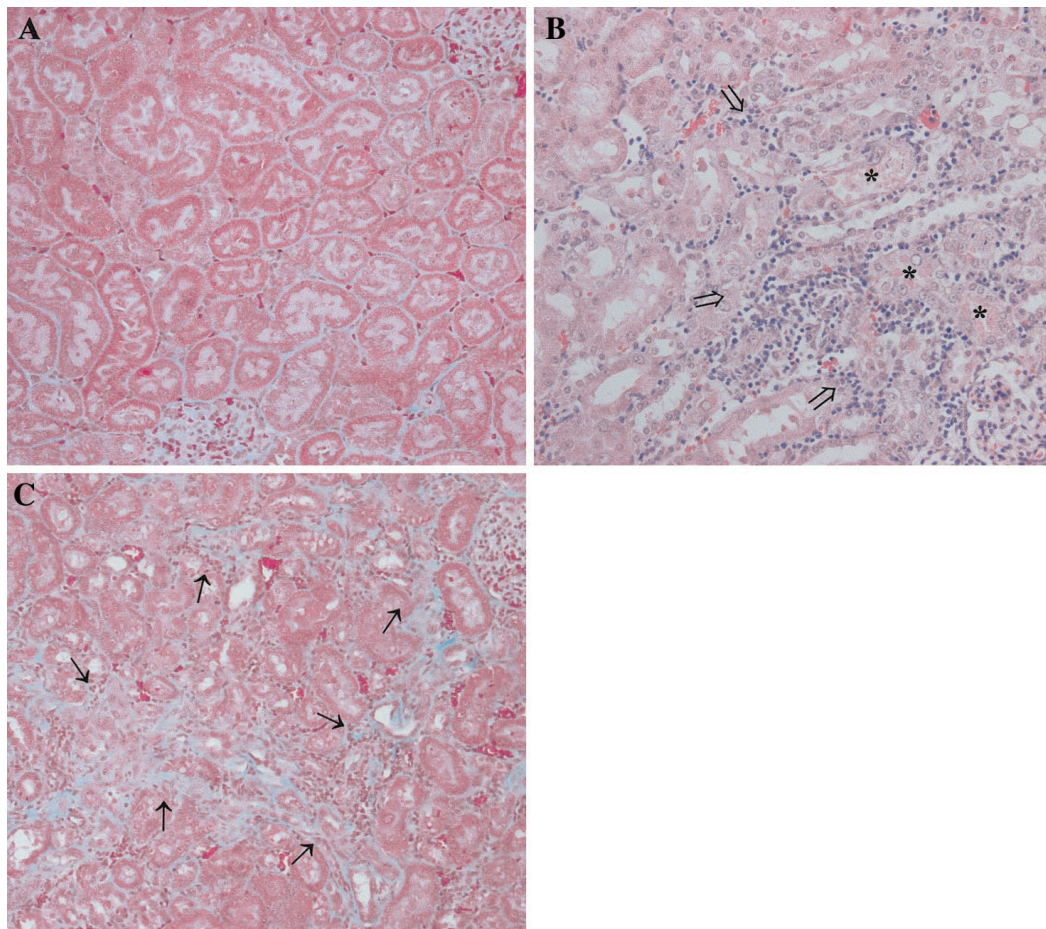


Figure 3. Photomicrographs of renal cortex. (A) For a control rat on day 35, no abnormalities were noted. Goldner's trichrome stain. Magnification, $\times 200$. (B) For a high-dose AA-treated (10 mg/kg body wt) rat on day 10, focal tubular necrosis (*) and an intense lymphocytic infiltrate (arrows) were observed. Hematoxylin and eosin. Magnification, $\times 200$. (C) For a high-dose AA-treated (10 mg/kg body wt) rat on day 35, severe tubular atrophy and interstitial fibrosis (arrows) were observed. Goldner's trichrome stain. Magnification, $\times 200$.

muscle cells of hilar arterioles or thickening of the intima and media of interlobular arteries, was not observed for any group.

Glomerular lesions were absent in the control and both AA groups. The lymphocytic infiltrates observed in high-dose AA-treated rats focally extended to the periglomerular interstitium, without affecting glomerular components.

Mean \pm SEM scores for tubular atrophy, tubular necrosis, lymphocytic infiltrates, and interstitial fibrosis were calculated from individual data collected for each group on days 10 and 35 (Figure 4). Significant tubular atrophy was present in all high-dose AA-treated animals on day 10 and persisted on day 35. Tubular necrosis was observed in high-dose AA-treated rats, with a maximum on day 10. Lymphocytic infiltrates were present in low- and high-dose AA groups on days 10 and 35. Interstitial fibrosis was intense in the high-dose AA group on day 35, whereas no trace could be detected in the low-dose AA and control groups.

Correlations between Tubulointerstitial Injuries and Biologic Parameters

Two structure-function relationships were assessed. The tubulointerstitial injury scores were closely correlated with se-

rum creatinine levels (Figure 5A) and negatively correlated with LAP enzymuria (Figure 5B).

Tumoral Lesions in AA-Treated Rats

Urothelial lesions were observed at different times in the study. In the low-dose AA group, two rats developed urothelial dysplasia on day 10 and two additional cases were observed later (two of six animals euthanized on day 105). In the high-dose AA group, urothelial dysplasia was detected on day 10 (two of six euthanized animals), on day 35 (one of six euthanized animals), and on day 105 (three of 11 euthanized animals). Moreover, three rats developed low-grade papillary urothelial carcinoma of the pelvis by day 105.

After day 35, voluminous tumors localized around the sites of subcutaneous injections (upper back) developed in the surviving AA-treated rats. Histologic examinations performed on day 105 demonstrated malignant fibrohistiocytic sarcoma in two of six euthanized animals in the low-dose AA group and in seven of 11 euthanized animals in the high-dose AA group.

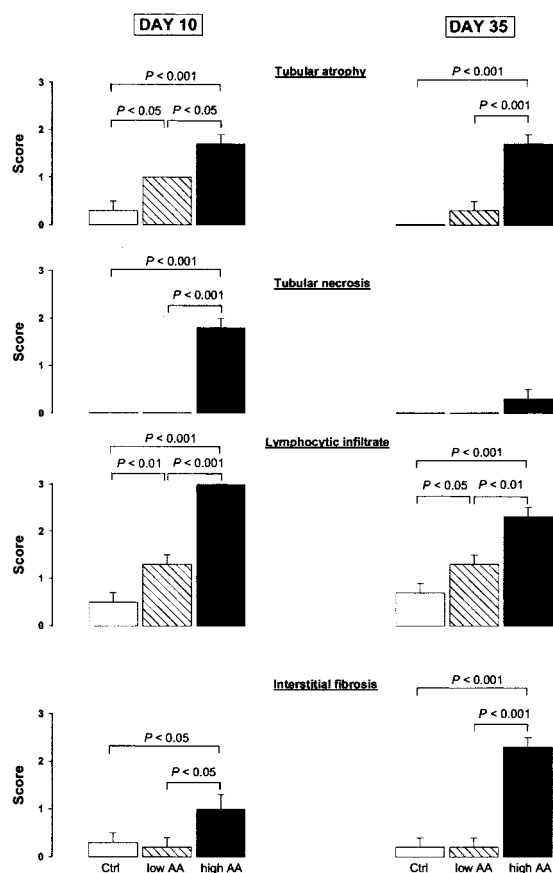


Figure 4. Semiquantitative tubulointerstitial scores for the control (□), low-dose AA (1 mg/kg body wt) (▨), and high-dose AA (10 mg/kg body wt) (■) groups on days 10 and 35. Data are the mean ± SEM for six rats/group.

Discussion

This report describes a short-term rat model, based on the model of cyclosporin-induced interstitial renal fibrosis in rats, that reproduces the main renal features of human CHN (renal failure, tubular atrophy, and interstitial fibrosis) after AA administration. To date, several findings have supported the involvement of AA in the pathogenesis of CHN. The replacement of *Stephania* by *Aristolochia* species was confirmed in different batches of powders delivered in Belgium under the name of *S. tetrandra*. Most of these batches contained not tetrandrine but AA (0.65 ± 0.56 mg/g) (2). The presence of 7-(desoxyadenosine- N^6 -yl)aristolactam I-DNA adducts was demonstrated in renal tissue samples obtained from patients with CHN, whereas 7-(desoxyadenosine- N^6 -yl)aristolactam I-DNA adducts were absent from the renal tissue of patients with other renal diseases (3,4).

However, the fact that AA itself could induce chronic renal failure via progressive interstitial fibrosis awaited experimental proof. Initial attempts to experimentally reproduce CHN failed. Two groups of seven rats were treated orally with either pure AA (10 mg/kg, 5 d/wk, for 3 mo) or herb powders (containing AA) mixed with fenfluramine. By the time of euthanasia, animals in both groups had developed the expected tumors but

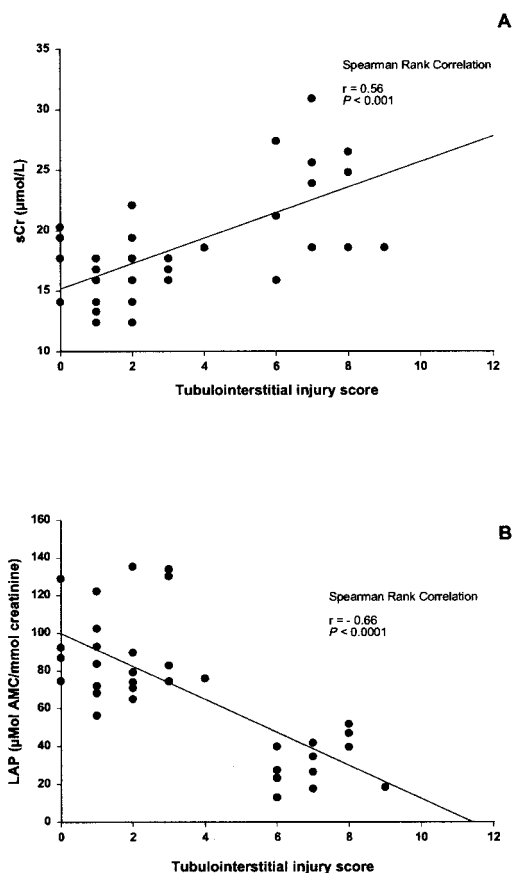


Figure 5. Correlations between tubulointerstitial injury scores and serum creatinine levels (sCr) (A) and LAP enzymuria (B) for all groups of rats, using individual histologic and biochemical data for days 10 and 35. AMC, 7-amido-4-methyl-coumarin.

no fibrosis of the renal interstitium (12). In contrast, when 12 female NZW rabbits were given intraperitoneal injections of 0.1 mg/kg AA (5 d/wk, for 17 to 21 mo), they developed severe hypocellular interstitial fibrosis, urothelial atypias, and, in three cases, tumors of the urinary tract (13).

This study demonstrates that, for successful production of a rat model of *Aristolochia* nephropathy, salt-depletion conditioning and a high dose of AA seem to be essential.

The salt depletion was used to enhance the onset of interstitial lesions via stimulation of the intrarenal angiotensin system, as reported for the cyclosporin A-induced nephropathy rat model (14,15,19).

The choice of AA dose was based on our clinical observations (1,2,4,5). With the assumptions of a maximal cumulative dose of *S. tetrandra* of 360 g, a maximal amount of AA of 1.56 mg/g of herb powder, and a body weight of 55 kg, the total amount of AA ingested by some patients was 10 mg AA/kg body wt, which represents a daily dose of 0.29 mg AA/kg body wt for 35 d.

Among the salt-depleted rats, only those treated with the high dose of AA, which was 30 times higher than that for CHN patients, developed renal interstitial fibrosis and renal failure within 35 d. Tubular atrophy and interstitial fibrosis were preferentially located in the deep cortex, as well as along the

medullary rays. This distribution of lesions is closer to histologic pattern I, as recently described for the NZW rabbit model (13). In addition to the morphologic findings, our biologic data (decreased LAP enzymuria and persisting glucosuria) support the hypothesis that proximal tubules may be a preferential target of AA toxicity (20).

Interestingly, interstitial fibrosis and tubular atrophy were preceded by an acute phase of tubular necrosis and lymphocytic infiltration (day 10). Early accumulation of immunocompetent cells in areas of active tubulointerstitial injury could be of major importance in the development of renal fibrosis. The involvement of mononuclear inflammatory cells in chronic renal scarring is recognized (21,22) and could explain some favorable results obtained with steroid treatment of patients with CHN (23). However, our data also confirm the carcinogenic properties of AA that were previously described (10,12), including the development of urothelial carcinoma.

In conclusion, salt-depleted male Wistar rats that received daily subcutaneous injections of AA at 10 mg/kg body wt developed interstitial renal fibrosis and chronic renal failure, as well as urothelial dysplasia, after 35 d. Taken together, these observations support the role of AA in the pathogenesis of human CHN. Finally, this short-term rat model may be useful for investigation of the mechanisms responsible for renal fibrosis.

Acknowledgments

Dr. Debelle is a research fellow of the Université Libre de Bruxelles (Brussels, Belgium). Our work was supported by grants from the Groupement pour l'Etude, le Traitement, et la Réhabilitation Sociale des Insuffisants Rénaux Chroniques, from the Fonds de la Recherche Scientifique Médicale (Belgium), and from the Fondation Erasme (Hôpital Erasme, Brussels, Belgium). We are indebted to Dr. Dany Mercan (Service de Chimie Médicale, Hôpital Erasme, Brussels, Belgium) for help with the development of the HPLC method to measure serum creatinine levels and to Dr. Alain Michel (University of Mons-Hainaut, Mons, Belgium) for analysis of the mixture of AA.

References

1. Vanherweghem JL, Depierreux M, Tielemans C, Abramowicz D, Dratwa M, Jadoul M, Richard C, Vandervelde D, Verbeelen D, Vanhaelen-Fastre R: Rapidly progressive interstitial renal fibrosis in young women: Association with slimming regimen including Chinese herbs. *Lancet* 341: 387–391, 1993
2. Vanhaelen M, Vanhaelen-Fastre R, But P, Vanherweghem JL: Identification of aristolochic acid in Chinese herbs. *Lancet* 343: 174, 1994
3. Schmeiser HH, Bieler CA, Wiessler M, Van Ypersele dS, Cosyns JP: Detection of DNA adducts formed by aristolochic acid in renal tissue from patients with Chinese herbs nephropathy. *Cancer Res* 56: 2025–2028, 1996
4. Nortier JL, Martinez MC, Schmeiser HH, Arlt VM, Bieler CA, Petein M, Depierreux MF, De Pauw L, Abramowicz D, Vereerstraeten P, Vanherweghem JL: Urothelial carcinoma associated with the use of a Chinese herb (*Aristolochia fangchi*). *N Engl J Med* 342: 1686–1692, 2000
5. Depierreux M, Van Damme B, Vanden Houte K, Vanherweghem JL: Pathologic aspects of a newly described nephropathy related to the prolonged use of Chinese herbs. *Am J Kidney Dis* 24: 172–180, 1994
6. Cosyns JP, Jadoul M, Squifflet JP, de Plaen JF, Ferluga D, Van Ypersele dS: Chinese herbs nephropathy: A clue to Balkan endemic nephropathy? *Kidney Int* 45: 1680–1688, 1994
7. Cosyns JP, Jadoul M, Squifflet JP, Wese FX, Van Ypersele dS: Urothelial lesions in Chinese-herb nephropathy. *Am J Kidney Dis* 33: 1011–1017, 1999
8. Schmeiser HH, Pool BL, Wiessler M: Identification and mutagenicity of metabolites of aristolochic acid formed by rat liver. *Carcinogenesis (Lond)* 7: 59–63, 1986
9. Mengs U: Acute toxicity of aristolochic acid in rodents. *Arch Toxicol* 59: 328–331, 1987
10. Mengs U, Lang W, Poch J-A: The carcinogenic action of aristolochic acid in rats. *Arch Toxicol* 57: 107–119, 1982
11. Mengs U: On the histopathogenesis of rat forestomach carcinoma caused by aristolochic acid. *Arch Toxicol* 52: 209–220, 1983
12. Cosyns JP, Goebbels RM, Liberton V, Schmeiser HH, Bieler CA, Bernard AM: Chinese herbs nephropathy-associated slimming regimen induces tumours in the forestomach but no interstitial nephropathy in rats. *Arch Toxicol* 72: 738–743, 1998
13. Cosyns JP, Dehoux JP, Guiot Y, Goebbels RM, Robert A, Bernard AM, Van Ypersele dS: Chronic aristolochic acid toxicity in rabbits: A model of Chinese herbs nephropathy? *Kidney Int* 59: 2164–2173, 2001
14. Young BA, Burdman EA, Johnson RJ, Alpers CE, Giachelli CM, Eng E, Andoh T, Bennett WM, Couser WG: Cellular proliferation and macrophage influx precede interstitial fibrosis in cyclosporine nephrotoxicity. *Kidney Int* 48: 439–448, 1995
15. Kon V, Hunley TE, Fogo A: Combined antagonism of endothelin A/B receptors links endothelin to vasoconstriction whereas angiotensin II effects fibrosis: Studies in chronic cyclosporine nephrotoxicity in rats. *Transplantation* 60: 89–95, 1995
16. Xue GP, Fishlock RC, Snoswell AM: Determination of creatinine in whole blood, plasma, and urine by high-performance liquid chromatography. *Anal Biochem* 171: 135–140, 1988
17. Bradford MM: A rapid and sensitive method for the quantitation of microgram quantities of protein utilizing the principle of protein-dye binding. *Anal Biochem* 72: 248–254, 1976
18. Epstein JI, Amin MB, Reuter VR, Mostofi FK: The World Health Organization/International Society of Urological Pathology consensus classification of urothelial (transitional cell) neoplasms of the urinary bladder: Bladder Consensus Conference Committee. *Am J Surg Pathol* 22: 1435–1448, 1998
19. Young BA, Burdman EA, Johnson RJ, Andoh T, Bennett WM, Couser WG, Alpers CE: Cyclosporine A induced arteriopathy in a rat model of chronic cyclosporine nephropathy. *Kidney Int* 48: 431–438, 1995
20. Nortier JL, Deschodt-Lanckman MM, Simon S, Thielemans NO, de Prez EG, Depierreux MF, Tielemans CL, Richard C, Lauwerys RR, Bernard AM, Vanherweghem JL: Proximal tubular injury in Chinese herbs nephropathy: Monitoring by neutral endopeptidase enzymuria. *Kidney Int* 51: 288–293, 1997
21. Muller GA, Schettler V, Muller CA, Strutz F: Prevention of progression of renal fibrosis: How far are we? *Kidney Int Suppl* 54: S75–S82, 1996
22. Rodriguez-Iturbe B, Pons H, Herrera-Acosta J, Johnson RJ: Role of immunocompetent cells in nonimmune renal diseases. *Kidney Int* 59: 1626–1640, 2001
23. Vanherweghem JL, Abramowicz D, Tielemans C, Depierreux M: Effects of steroids on the progression of renal failure in chronic interstitial renal fibrosis: A pilot study in Chinese herbs nephropathy. *Am J Kidney Dis* 27: 209–215, 1996